https://doi.org/10.1093/plphys/kiad136 PLANT PHYSIOLOGY 2023: 1–17

Plant Physiology®

Research Article

Rice HEAT SHOCK PROTEIN60-3B maintains male fertility under high temperature by starch granule biogenesis

Sen Lin,[1,†] Ze Liu,[1,†] Shiyu Sun,[1] Feiyang Xue,[1] Huanjun Li,[1] Askar Tursun,[1] Lichun Cao,[1] Long Zhang,[2] Zoe A. Wilson,[3] Dabing Zhang[1,4] and Wanqi Liang[1,*]

1 Joint International Research Laboratory of Metabolic and Developmental Sciences, State Key Laboratory of Hybrid Rice, School of Life Sciences and Biotechnology, Shanghai Jiao Tong University, Shanghai 200240, China
2 Key Laboratory of Crop Genetics and Physiology of Jiangsu Province, Jiangsu Key Laboratory of Crop Genomics and Molecular Breeding, Yangzhou University, Yangzhou 225009, China
3 Division of Plant & Crop Sciences, School of Biosciences, University of Nottingham, Sutton Bonington Campus, Loughborough, Leicestershire LE12 5RD, UK
4 School of Agriculture, Food and Wine, University of Adelaide, Waite Campus, Glen Osmond, South Australia 5064, Australia

*Author for correspondence: wqliang@sjtu.edu.cn
†These authors contributed equally to this work.
The author responsible for distribution of materials integral to the findings presented in this article in accordance with the policy described in the Instructions for Authors (https://academic.oup.com/plphys/pages/General-Instructions) is Wanqi Liang.

Abstract

Heat stress has a deleterious effect on male fertility in rice (*Oryza sativa*), but mechanisms to protect against heat stress in rice male gametophytes are poorly understood. Here, we have isolated and characterized a heat-sensitive male-sterile rice mutant, *heat shock protein60-3b* (*oshsp60-3b*), that shows normal fertility at optimal temperatures but decreasing fertility as temperatures increase. High temperatures interfered with pollen starch granule formation and reactive oxygen species (ROS) scavenging in *oshsp60-3b* anthers, leading to cell death and pollen abortion. In line with the mutant phenotypes, *OsHSP60-3B* was rapidly upregulated in response to heat shock and its protein products were localized to the plastid. Critically, overexpression of *OsHSP60-3B* enhanced the heat tolerance of pollen in transgenic plants. We demonstrated that OsHSP60-3B interacted with FLOURY ENDOSPERM6(FLO6) in plastids, a key component involved in the starch granule formation in the rice pollen. Western blot results showed that FLO6 level was substantially decreased in *oshsp60-3b* anthers at high temperature, indicating that OsHSP60-3B is required to stabilize FLO6 when temperatures exceed optimal conditions. We suggest that in response to high temperature, OsHSP60-3B interacts with FLO6 to regulate starch granule biogenesis in rice pollen and attenuates ROS levels in anthers to ensure normal male gametophyte development in rice.

Introduction

Plants adapt to their changeable environment by mobilizing physiological and morphological responses but can be highly susceptible to increasingly common environmental stresses, such as heat. Even mild elevated temperatures, particularly in the vulnerable reproductive stages, can be a substantial threat to crop yield. For example, rice (*Oryza sativa*) yield has been reported to drop by 10% for every 1°C increase in ambient temperature during reproductive growth (Peng et al. 2004), while wheat (*Triticum aestivum*) yield drops by 5% for every 1°C over 21°C daytime and 16°C nighttime temperatures (Tashiro and Wardlaw 1989).

In cereal crops, male reproduction is most sensitive to temperature stresses (Zinn et al. 2010). Pollen, the male gametophyte, is produced in anthers where microsporocytes

Received October 04, 2022. Accepted January 29, 2023. Advance access publication March 2, 2023

(diploid pollen mother cells) undergo meiosis to produce four haploid microspores (tetrad), which undergo mitosis to produce viable mature pollen filled with starch and lipids (Zhang et al. 2011; Hafidh et al. 2016). Heat stress affects several aspects of anther and pollen development, especially meiosis, tapetal programmed cell death, and cellular metabolism (Lohani et al. 2020). During late development, microspores accumulate large reserves of carbohydrates and lipids essential for pollen viability; rice mutants lacking starch in the pollen are male-sterile (Mu et al. 2009; Lee et al. 2016). In rice, starch begins to accumulate after the first microspore mitosis, and large numbers of starch granules are observed in mature pollen (Zhang et al. 2021). Abiotic stresses, including heat, commonly induce decreased accumulation of sugar and starch in pollen, which has been considered a predominant factor causing male sterility (De Storme and Geelen 2014), and heat-tolerant genotypes normally retain higher levels of pollen carbohydrates compared with heat-sensitive genotypes (Pressman 2002; Firon et al. 2006). However, whether the reduction in carbohydrate levels is the primary reason for stress-induced male sterility or an indirect consequence of pollen dysfunction remains unclear.

High temperatures trigger the heat stress response in plants, a series of highly conserved physiological and molecular processes (Chaturvedi et al. 2021) affecting enzyme activity (Wang et al. 2015; Ji et al. 2021); microtubule organization (Song et al. 2020); membrane permeability and fluidity (Sangwan et al. 2002); thylakoid stability (Yu et al. 2012b); photosynthetic activity (Crafts-Brandner and Salvucci 2000); and the production of denatured proteins and Ca^{2+}-dependent signaling through the plasma membrane (Ohama et al. 2017). Heat stress can induce transcriptional regulation of *HEAT SHOCK PROTEINS* (*HSPs*) by activating heat shock transcription factors (HSF; Ohama et al. 2017). Reactive oxygen species (ROS), plant metabolic and signaling molecules such as hydrogen peroxide, also accumulate when cells perceive the heat stress signal (Song et al. 2020). Plants mobilize reserves of antioxidant metabolites to correct oxidative damage induced by ROS to avoid cell death under heat shock (Larkindale and Knight 2002).

HSPs exist in all cellular organisms and are highly conserved (Ziningа et al. 2021); they comprise up to 10% of the total protein in human cells (Finka et al. 2016). HSPs play crucial roles in protein folding, unfolding, sorting, and transmembrane transport and assembly under stress and non-stress conditions (Usman et al. 2014; Finka et al. 2016). Induction of HSPs by heat and other stresses is required to maintain proper protein conformation by preventing misfolding and aberrant aggregation, thus ensuring cellular homeostasis (Usman et al. 2014). HSPs are generally divided into five major families based on molecular weight: HSP100, HSP90, HSP70, HSP60, and sHSP/α-crystallins (Tissières et al. 1974). HSP60 proteins can be further divided into Group I and Group II chaperonins: Group I chaperonins include GROWTH ESSENTIAL LARGE (GroEL) in eubacteria and HSP60s in chloroplasts and mitochondria, while Group II chaperonins include HSP60 in archaea and the eukaryotic cytosol (Hill and Hemmingsen 2001).

In plants, the chloroplast-localized HSP60s (CHAPERONIN PROTEIN60; CPN60s) are critical for chloroplast function as well as various developmental processes. CPN60 was identified as a homolog of GroEL that aids assembly of Rubisco, a key enzyme in photosynthesis (Hemmingsen et al. 1988). CPN60 consists of two subunits, CPN60α and CPN60β, that share ∼50% sequence similarity. The Arabidopsis (*Arabidopsis thaliana*) genome contains two *CPN60α* and four *CPN60β* genes, which have redundant or divergent roles in chloroplast functioning, embryo development, and flowering time control (Apuya et al. 2001; Suzuki et al. 2009; Ke et al. 2017; Tiwari and Grover 2019). Rice has three *CPN60α* and three *CPN60β* genes in its genome (Kim et al. 2013; Jiang et al. 2014), and *OsCPN60α1*, *OsCPN60α2/THERMOSENSITIVE CHLOROPLAST DEVELOPMENT (TCD) 9* and *OsCPN60β1* are required for chloroplast development and early plant growth (Kim et al. 2013; Jiang et al. 2014; Wu et al. 2020). However, functions of other HSP60s remain largely unknown.

In this study, we report the discovery and characterization of rice *HSP60-3B* (LOC_Os10g32550), which protects pollen development at high temperatures (>34°C) by regulating starch accumulation and ROS levels. At low temperatures (22∼28°C), *oshsp60-3b* plants resemble wild type, but as temperature increases, *oshsp60-3b* pollen exhibit compromised starch accumulation and decreased viability, while anthers produce elevated ROS levels with concomitant increases in cell death. We demonstrate that the heat-induced OsHSP60 mediates pollen starch granule formation at high temperature by interacting and stabilizing the starch-binding protein FLOURY ENDOSPERM6 (FLO6, Zhang et al. 2022b). Our study provides insights into how rice plants can maintain fertility under elevated temperatures.

Results

oshsp60-3b is a temperature-sensitive male-sterile mutant

To identify genes involved in heat stress tolerance during rice male reproduction, we isolated a heat-sensitive, male-sterile mutant from our existing library (Chen et al. 2006). Map-based cloning and sequencing identified the gene as a member of the heat shock protein (HSP) 60 family with homology to the Arabidopsis HSP60-3B protein (described in a subsequent section); for convenience, we will use the *oshsp60-3b* nomenclature from the beginning to refer to our gene of interest.

At mild growth temperatures (25 to 32°C) in the paddy field during summer in Shanghai, *oshsp60-3b* and wild type (WT) plants exhibited normal flower development (Supplemental Fig. S1, A and B). However, *oshsp60-3b* flowers had paler yellow anthers that produced some sterile pollen grains (Supplemental Fig. S1, C to J). When WT pollen grains were used to fertilize *oshsp60-3b* stigma, the resulting

spikelets showed normal development and F_1 progeny exhibited a normal phenotype, indicating that the female organ of *oshsp60-3b* is functional and that the *oshsp60-3b* mutation is recessive (Supplemental Fig. S2).

To examine how temperature affects the fertility of *oshsp60-3b*, we grew plants at several different temperatures: low (22°C), mid (28°C), and high (34°C; Supplemental Table S1). WT anthers were bright yellow at all three temperatures, and mature pollen grains were round and viable (Fig. 1, A to C, G to I). Consistent with field observations, *oshsp60-3b* displayed normal flower development and fertility at low temperatures (Fig. 1, D, J, M, and N), but as the temperature increased to 28°C, anthers became paler and mature pollen grains were partially sterile (Fig. 1, E, K, and M). The seed setting ratio also decreased (Fig. 1N). At 34°C, *oshsp60-3b* anthers were white and stunted, and the mature

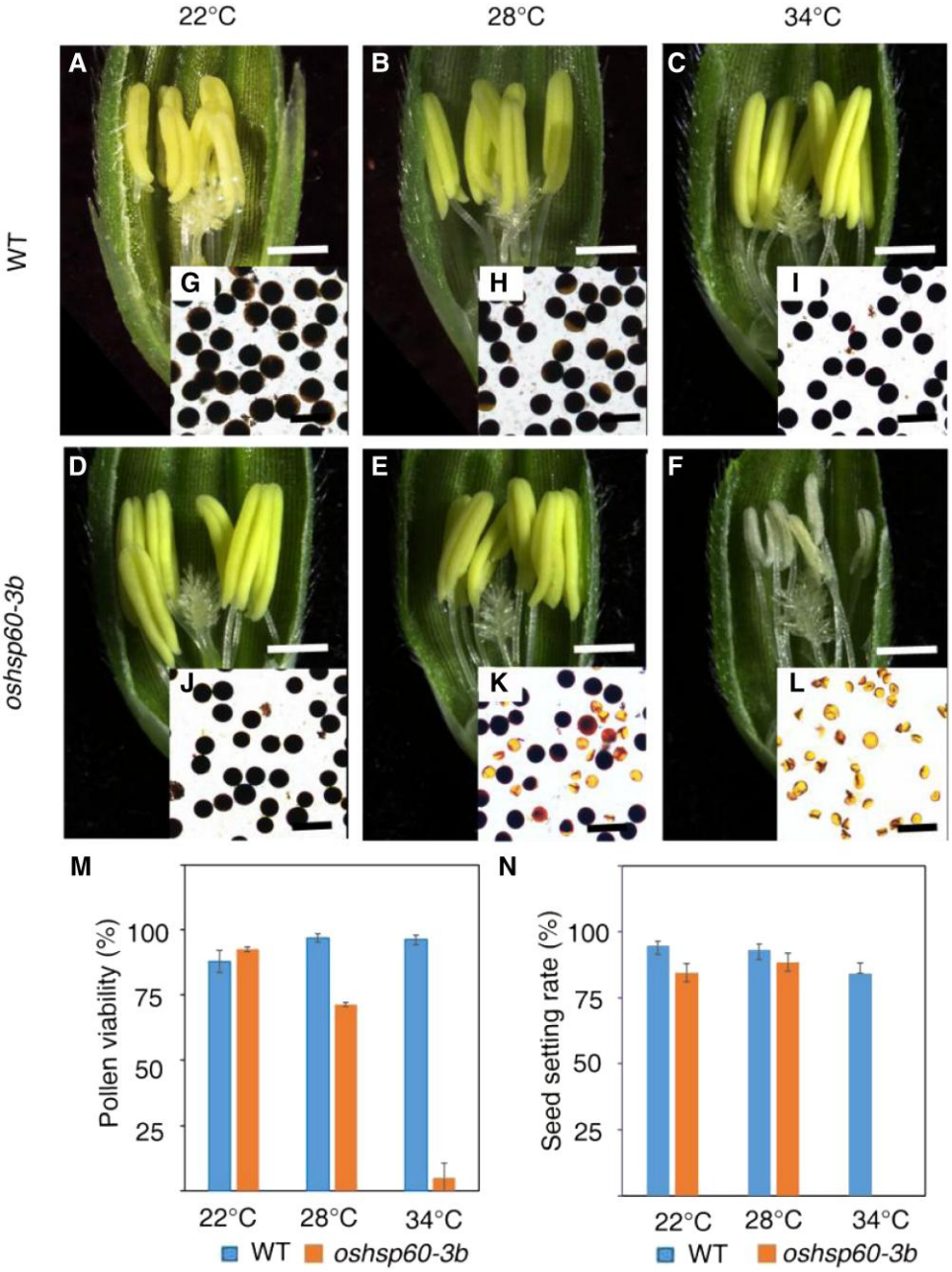

Figure 1. Male fertility of *oshsp60-3b* is compromised under high temperature. **A** to **F**, Wild-type (WT) and *oshsp60-3b* mutant spikelets at Stage 13. Spikelets shown after removal of half the lemma and palea. Bars, 1 mm. Anthers in *oshsp60-3b* look normal at 22°C and 28°C, but become small and white at 34°C. **G** to **L**, Pollen grain from the shown spikelet stained with iodine–potassium iodide (I_2–KI), where dark staining indicates viable pollen. Bars, 100 μm. **M**, Viability of WT and *oshsp60-3b* pollen at different temperatures. Mean ± SD, $n = 10$. Pollen viability is decreased at 28°C and abolished at 34°C in *oshsp60-3b*. **N**, Seed setting rate of WT and *oshsp60-3b* plants at different temperatures. Mean ± SD, $n = 10$. *oshsp60-3b* plants exhibit normal seed setting at 22°C and 28°C, but set no seed at 34°C.

pollen grains were sterile and could not set seed (Fig. 1, F, L, M, and N).

OsHSP60-3B is required for pollen development at high temperature

To explore the cytological defects of *oshsp60-3b*, transverse sections of anthers grown at the three different temperatures were observed. No obvious differences were observed from Stages 9 to 11 of *oshsp60-3b* anther development (Fig. 2A; stages of anther development taken from Zhang and Wilson 2009; Zhang et al. 2011), indicating that meiosis and mitosis occur normally in *oshsp60-3b* anthers. Accordingly, chromosome behavior was observed to undergo a normal meiotic process in *oshsp60-3b* anthers at 34°C, as evidenced by the normal formation of tetrads that each contained four young microspores (Supplemental Fig. S3). At S12, WT anthers produced large, round mature pollen grains at all temperatures, while *oshsp60-3b* showed a similar phenotype at 22°C, approximately half of the *oshsp60-3b* pollen grains at 28°C were abnormal (small and shrunken), and all *oshsp60-3b* pollen grains were aborted at 34°C (Fig. 2, A and B). WT plants exhibited normal development at all temperatures, so only wild-type phenotypes at 34°C are shown in the following figures unless it is specifically pointed out.

Transmission electron microscopy (TEM) confirmed that, from Stages 8 to 10, WT and *oshsp60-3b* anthers at high temperature formed tetrads, released free microspores, and became vacuolated (Supplemental Fig. S4). By S12 (pollen maturity), WT anthers formed large, round, mature pollen grains filled with large starch granules and were enclosed in a thick intine layer (Fig. 3). *oshsp60-3b* pollen at 22°C was similar to WT; at 28°C, pollen grains developed abnormally and contained smaller starch granules; and at 34°C, pollen grains were empty and surrounded by much thinner intine, suggesting that the microspore development was affected at late stage (Fig. 3). To further study the phenotype of *oshsp60-3b*, scanning electron microscopy (SEM) of the surfaces of S12 WT and *oshsp60-3b* anthers and pollen grains at different temperatures was performed (Supplemental Fig. S5). The spaghetti-like cuticle on the anther epidermis, the crystal-like Ubisch bodies on the inner surface of anther, and sporopollenin in the exine of pollen grains of *oshsp60-3b* mutants resembled WT at all three temperatures (Supplemental Fig. S5).

Thus, the only difference between WT and *oshsp60-3b* pollen was that, as the temperature rose, so did the proportion of deflated, sterile pollen grains, so that *oshsp60-3b* pollen was sterile when grown at 34°C (Fig. 2, A and B). These observations implied that *OsHSP60-3B* is required for pollen development, filling, and maturation at high temperatures.

OsHSP60-3B encodes a HEAT SHOCK 60 protein

To identify the gene underlying the *oshsp60-3b* mutation, we employed a map-based cloning strategy using an F_2 population derived from crossing the mutant line (japonica) with an indica cultivar. Using five InDel markers, the region was

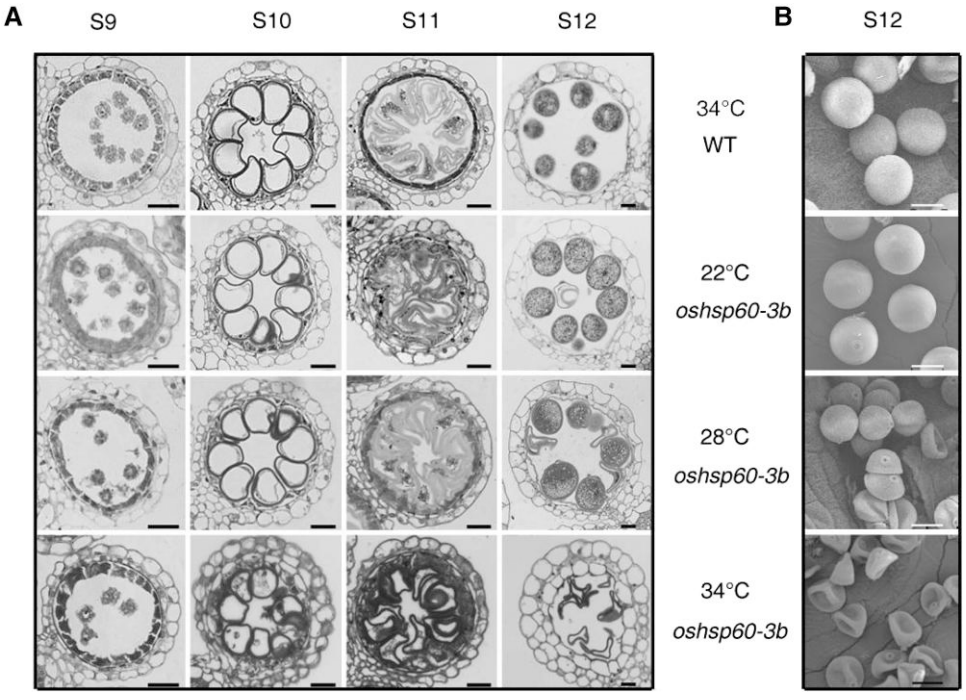

Figure 2. *Oshsp60-3b* mutant anthers display temperature-dependent male sterility. **A**, Transverse semi-thin sections of WT anthers at 34°C and *oshsp60-3b* anthers at 22°C, 28°C, and 34°C from Stages 9 to 12. Bars, 20 μm. Shrunken pollen grains are observed in *oshsp60-3b* at 28°C and 34°C to different extent. **B**, Scanning electron micrographs of mature (S12) WT and *oshsp60-3b* pollen grains at 22°C, 28°C, and 34°C. Bars, 20 μm. Pollen grains in *oshsp60-3b* exhibit normal morphology at 22°C, become partially aberrant at 28°C, and are all shrunken at 34°C.

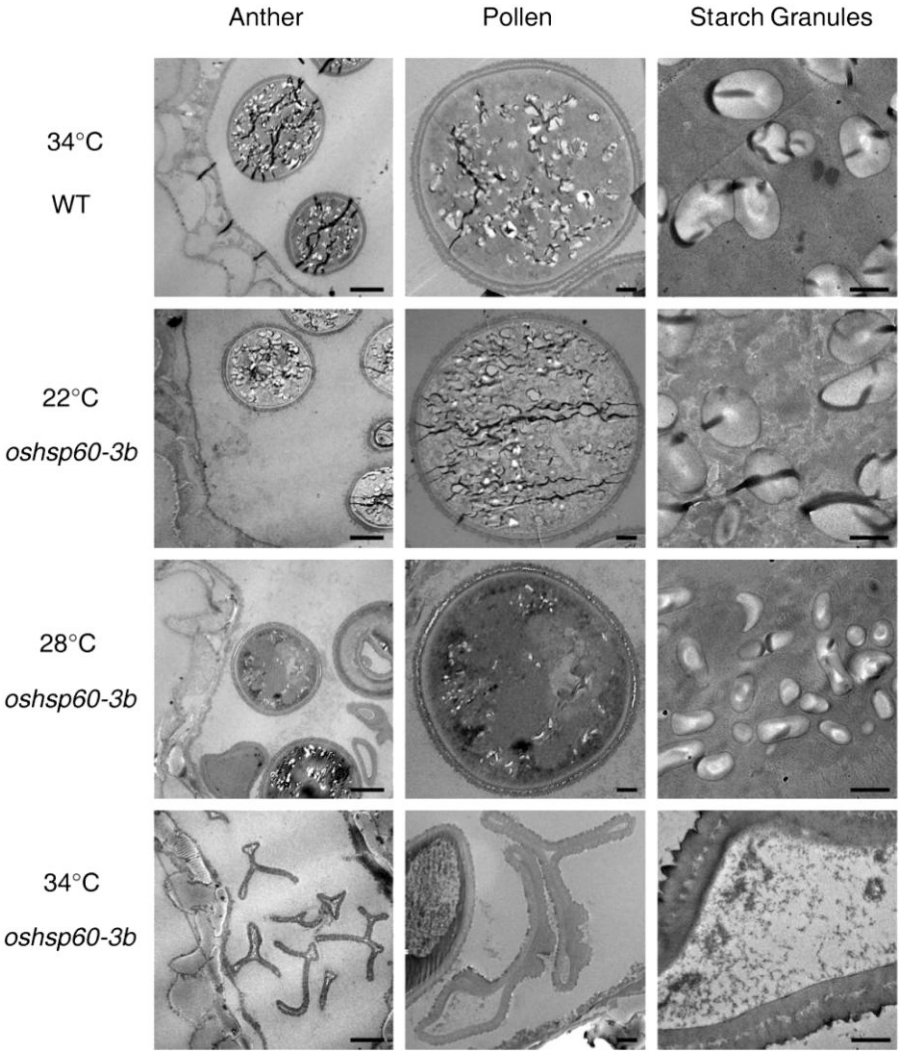

Figure 3. Starch granule formation is impaired in *oshsp60-3b* at high temperature. Transmission electron microscopy of S12 WT and *oshsp60-3b* anthers, pollen, and starch granules at different temperatures. In the *oshsp60-3b* pollen, starch granules become much smaller at 28°C and disappear at 34°C. Bars: anthers, 10 μm; pollen, 2.5 μm; pollen contents, 1 μm.

narrowed to 210 kb between markers AC068951-3 and AC022457 on chromosome 10 (Fig. 4A), a region covered by three bacterial artificial chromosome clones. High-throughput resequencing using a mixed mutant population sample was used to identify the gene and causative mutation as an 8 bp deletion in exon 17 of LOC_Os10g32550 (annotated OsHSP60 in www.gramene.org/), leading to a frame shift that resulted in a protein with 79 mutant amino acids at its C-terminus (Fig. 4, B and C).

To confirm gene identity, CRISPR-Cas9 technology was used to generate nonfunctional OsHSP60-3B proteins. Two new mutant alleles were produced: *oshsp60-3b-c1* with a 1 bp insertion in exon 3 that immediately created a new stop codon, while *oshsp60-3b-c2* had a 2 bp deletion in exon 13 leading to a frame shift that created a short 12 aa mutant sequence before a new stop codon (Supplemental Fig. S6A). The *oshsp60-3b-c1* and *oshsp60-3b-c2* mutants showed similar phenotypes to the original *oshsp60-3b* mutant, with partial sterility at 28°C, and sterility at 34°C (Fig. 1; Supplemental Fig. S6B).

Complementation of the *oshsp60-3b* mutant with the WT genomic *OsHSP60-3B* sequence driven by its native promoter (*pOsHSP60-3B::OsHSP60-3BgDNA*) was used to confirm the identity of the causative mutation. Transgenic plants showed rescue of the mutant phenotype at 34°C (Supplemental Fig. S7), confirming that the mutation in LOC_Os010g32550 is responsible for the temperature-sensitive male-sterile phenotype in *oshsp60-3b*.

LOC_Os10g32550 is predicted to encode a 634 aa protein across 18 exons that contains a putative HSP60-TCP1 domain (Fig. 4B). A phylogenetic analysis, based on its HSP60-TCP1 domain, identified fourteen Arabidopsis and 10 rice homologs from public databases, with LOC_Os10g32550 most similar to AtHSP60-3B (Fig. 4D). Three rice proteins with HSP60-TCP1 domains have been reported with roles in heat-dependent chloroplast or general

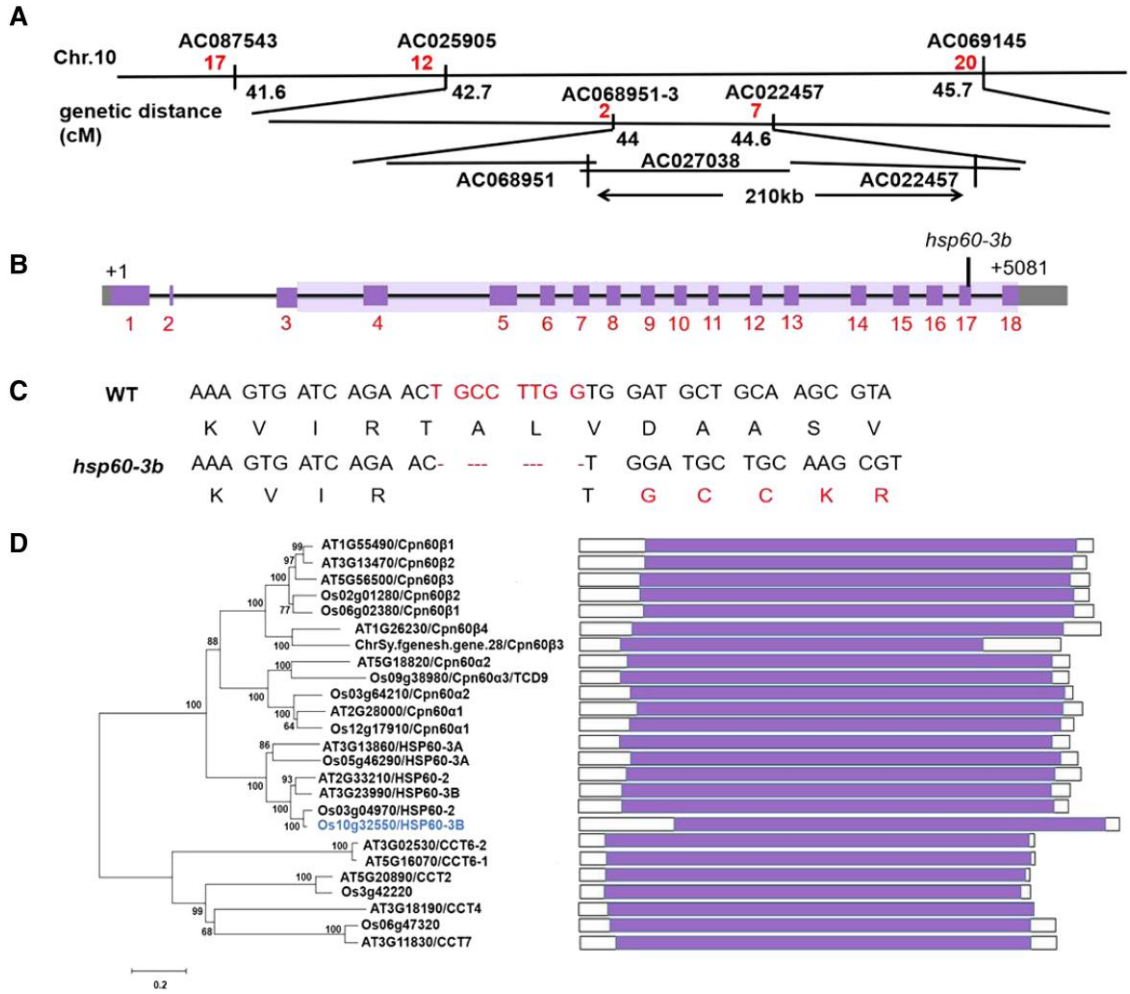

Figure 4. Map-based cloning and analysis of *OsHSP60-3B*. **A**, Fine mapping of *OsHSP60-3B* (LOC_Os10g32550) on chromosome 10. Names and positions of the molecular markers are shown. Numbers in red indicate the number of recombinants identified in the F_2 population. **B**, A schematic representation of *OsHSP60-3B* gene structure; numbered purple boxes indicate exons, and intervening black lines indicate introns. Gray boxes represent untranslated regions. The light purple shaded area indicates the TCP1-1/CPN60 chaperonin domain. +1 indicates the beginning of the translational start site (ATG), and +5081 indicates the end of the stop codon (TAG). The location of the mutation in exon 17 is indicated. **C**, The *oshsp60-3b* mutant has an 8 bp deletion in exon 17, leading to a frameshift. **D**, A neighbor-joining tree was constructed using MEGA with OsHSP60-3B proteins containing a TCP1-1/CPN60 chaperonin domain from aa 114 to 617 in rice (Os, 10 proteins) and Arabidopsis (AT, 14 proteins). OsHSP60-3B is highlighted. Bootstrap values in percentage (1,000 replicates) are indicated on the nodes. The scale bar, 0.2 phylogenetic distance.

plastid development during early vegetative growth (TCD9 (Jiang et al. 2014); OsCPN60α1 (Kim et al. 2013); and OsCPN60β1 (Wu et al. 2020)), suggesting that OsHSP60-3B may be also involved in plastid development.

OsHSP60-3B is widely expressed and localized to plastids

OsHSP60-3B expression was examined in various rice reproductive and vegetative rice tissues. *OsHSP60-3B* was expressed in anthers from Stages 6 to 13, as well as in root, stem, leaf, and palea/lemma tissues (Fig. 5A). To determine more precisely the spatial and temporal patterns of *OsHSP60-3B* expression, we introduced a construct containing the *GUS* reporter gene driven by the 2.9 kb *OsHSP60-3B* promoter (*pOsHSP60-3B*) into WT plants. GUS signals were detectable in the anther at Stages 9 to 13 (Fig. 5B), which was generally consistent with RT-qPCR data (Fig. 5A). Within transgenic anthers, *OsHSP60-3B* was expressed in microspores and mature pollen grains (Fig. 5C). Although highly expressed in vegetative tissues (Fig. 5A), *oshsp60-3b* did not show obvious defects during vegetative growth, suggesting that there might be other HSP60 proteins sharing redundant roles with OsHSP60-3B.

To examine whether *OsHSP60-3B* expression is induced by heat, we subjected WT and *oshsp60-3b* seedlings grown at 28°C to a 3 h heat shock at 42°C. Within 0.25 h, *OsHSP60-3B* mRNA levels increased significantly in WT leaves (Fig. 5D). After 0.25 h of heat shock, *OsHSP60-3B* expression began to decrease, dropping to original expression levels after ~3 h of heat shock prior to recovery at 28°C.

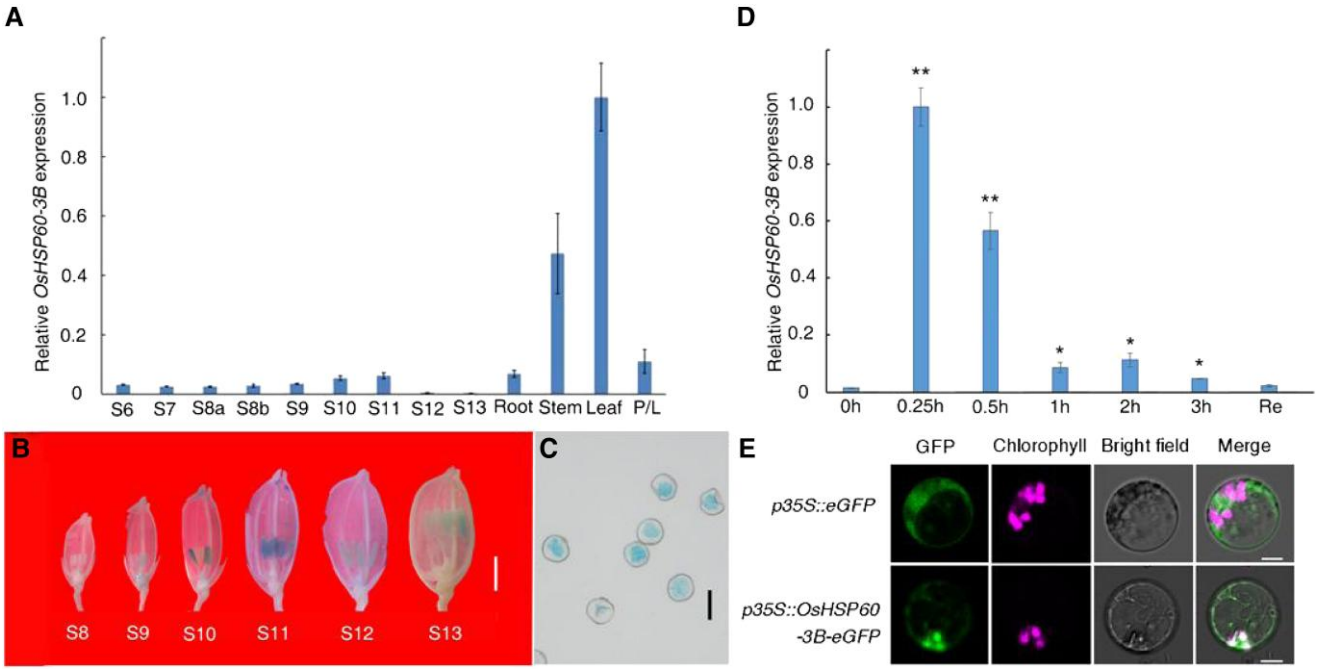

Figure 5. *OsHSP60-3B* is widely expressed and OsHSP60-3B is localized to the plastid. **A**, *OsHSP60-3B* expression in root, stem, leaf, palea/lemma (P/L), and anthers at different developmental stages (Supplemental S6 to S13) under normal conditions, relative to OsActin in the same tissue. Mean ± SD, $n = 3$. **B**, GUS expression in anthers of the *pOsHSP60-3B::GUS* transgenic plant at various stages. Bar, 1 mm. GUS signals are observed in anthers from Stage 9 to Stage 13. The individual anthers were digitally extracted for comparison. **C**, GUS expression in the microspore at Stage 11. Bar, 20 μm. **D**, Expression of *OsHSP60-3B* in response to heat stress relative to OsActin in the same tissue. WT seedlings (14 d) grown in rice culture solution at 28 °C were subjected to heat stress at 42°C. Their third leaves were sampled during treatment (0.25, 0.5, 1, 2, and 3 h) and after 2 h of recovery at 28°C (Re). Mean ± SD, $n = 3$. * $P < 0.05$; ** $P < 0.01$ (Student's *t*-test). **E**, Subcellular localization of OsHSP60-3B-eGFP in rice protoplasts showing co-location of OsHSP60-3B with plastids. Confocal micrographs were taken 16 h after transformation. Bars, 4 μm.

Protein localization was determined using a constitutively expressed eGFP-tagged OsHSP60-3B construct (*p35S::OsHSP60-3B-eGFP*) transiently expressed in Arabidopsis and rice protoplasts. The GFP signal mainly overlapped with auto-fluorescence of chloroplasts (Fig. 5E, Supplemental Fig. S8), indicating that OsHSP60-3B localizes to plastids. Like other rice HSP60-TCP1 domain proteins, OsHSP60-3B may regulate plastid development, but with an additional, unusual role in reproductive development.

OsHSP60-3B regulates pollen starch granule development by interacting with FLO6

Based on the defective starch accumulation in late stage *oshsp60-3b* anthers at high temperature, we hypothesized that OsHSP60-3B may play an important role in starch synthesis. Because HSP family proteins can act as chaperones that direct correct protein folding and function under stress conditions, we examined whether OsHSP60-3B affects starch synthesis by interacting with essential protein(s). To identify proteins that may interact with OsHSP60-3B, a yeast-two-hybrid (Y2H) screen in 5 to 7 mm anthers was performed using full-length OsHSP60-3B as bait. Only one plastid-localized protein, FLO6, was identified among the candidate proteins. FLO6 contains the carbohydrate-binding module (CBM) 48 domain and has been reported to direct starch synthesis in rice anther and endosperm (Peng et al. 2014; Zhang et al. 2022b). A pairwise Y2H verified that OsHSP60-3B can interact with FLO6 (Fig. 6A). Split-luciferase and bimolecular fluorescence complementation (BiFC) assays confirmed the interaction between HSP60-3B and FLO6 proteins in tobacco (*Nicotiana tabacum*) leaves (Fig. 6, B and C). A western blot assay indicated that the amount of the FLO6 protein decreased dramatically at S12 in *oshsp60-3b* compared with WT anthers at high temperatures (Fig. 6D), confirming a physiological link between these two proteins in rice.

OsHSP60-3B affects male fertility by regulating HSP and HSF genes and ROS levels

To further explore the *OsHSP60-3B* regulatory network, WT and *oshsp60-3b* anthers grown at 34°C were subjected to RNA sequencing at three stages of development (S10–12). A total of 9,363 differentially expressed genes (DEGs) were identified using $|\log_2 \text{fold change}| \geq 1$ and false discovery rate (FDR) < 0.05 (Supplemental Tables S2 to S4). Two hundred and ninety-eight genes were differently expressed at all three stages in *oshsp60-3b* and WT anthers (Fig. 7A). Many genes were upregulated at S12 in both the WT and especially *oshsp60-3b* anthers (Fig. 7B). Among the DEGs, many HSPs and HSFs were upregulated in *oshsp60-3b* anthers at

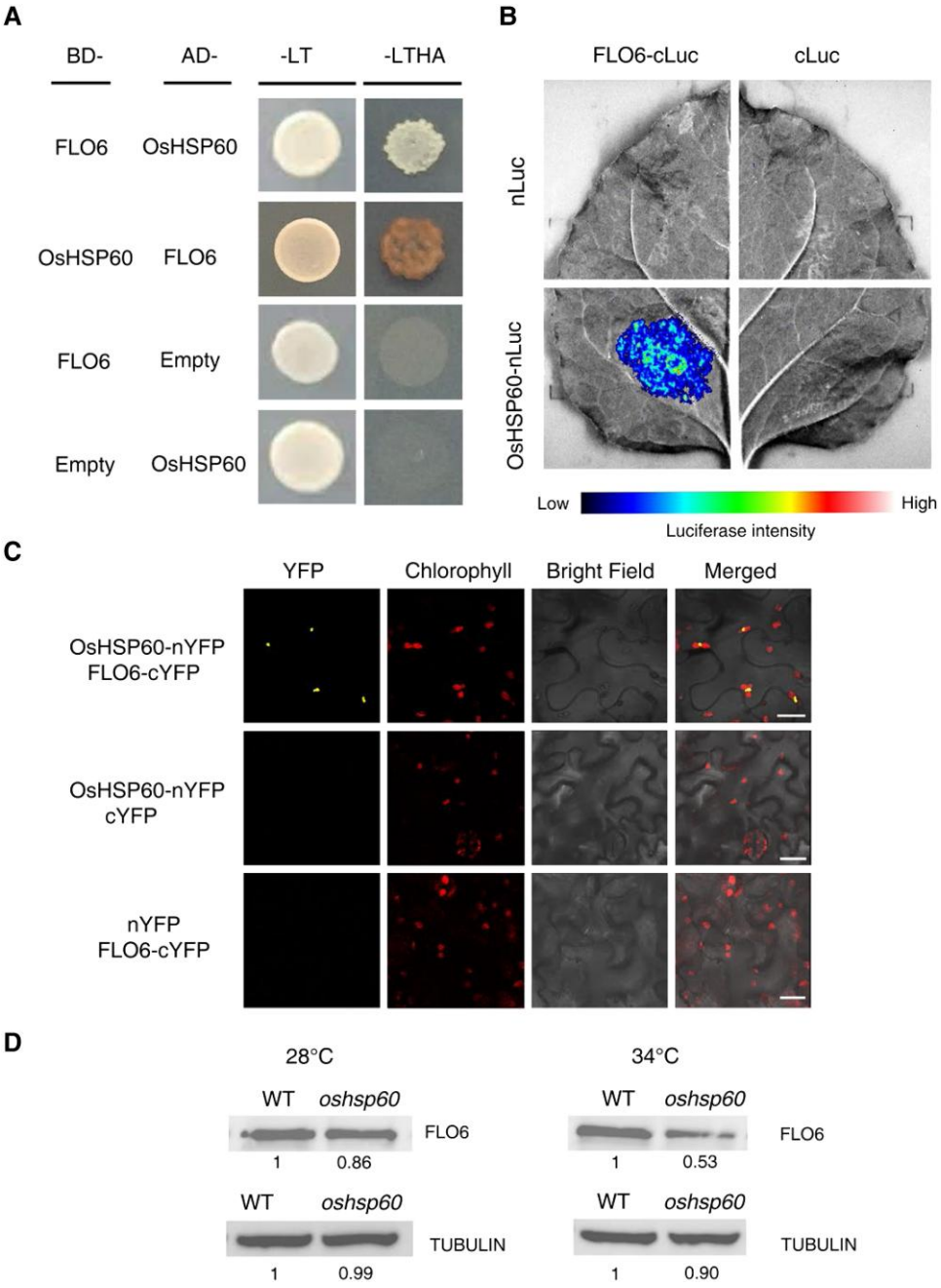

Figure 6. OsHSP60-3B interacts with and stabilizes FLO6. **A**, Y2H assays using HSP60-3B and FLO6 fused to either the GAL4 activation domain (AD) or binding domain (BD) and tested together or with negative controls. Medium −LT (SD-Leu/-Trp) was used to test for the presence of co-transformed plasmids; medium −LTHA (SD-Leu/-Trp/-His/-Ade) was used to test for protein interactions. **B**, Split-luciferase assays using HSP60-3B, FLO6, and controls in *Nicotiana tabacum* leaves. cLuc, C-terminal luciferase; nLuc, N-terminal luciferase. Strong luciferase signals are observed in the area infiltrated with OsHSP60-3B-nluc and FLO6-cluc. **C**, Bifluorescence complementation (BiFC) assay between HSP60-3B and FLO6 in *Nicotiana tabacum* leaf epidermal cells. Bars, 25 μm. YFP signals are only observed in the chloroplasts of leaves infiltrated with OsHSP60-3B-nYFP and FLO6-cYFP. **D**, FLO6 protein level is substantially decreased in *oshsp60-3b* anthers at 28°C and 34°C. Tubulin was used as a loading control. Numbers indicate relative band intensities.

S10–12 (Supplemental Fig. S9). Gene Ontology (GO) analysis identified 40 biological process (BP) and molecular function (MF) categories enriched in DEGs at S10; 88 at S11; and 175 at S12 (Supplemental Tables S5 to S7).

Heat stress can cause accumulation of ROS in plants (Chen et al. 2022), so we also examined ROS-related genes. GO pathway annotations confirmed that oxidation–reduction was the most enriched biological process at all three stages. Response to oxidative stress also was enriched at S12. Oxidoreductase activity was the most enriched molecular function at all three stages, while peroxidase activity and oxidoreductase activity, acting on peroxide as acceptor, were

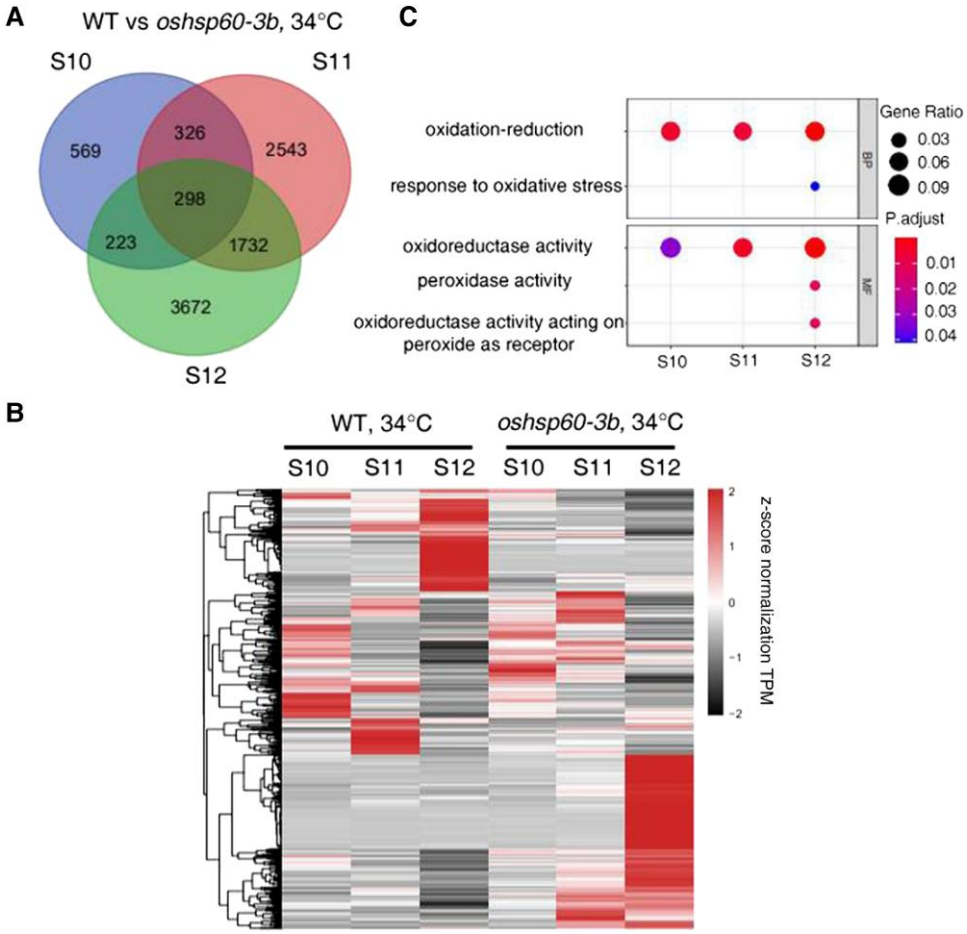

Figure 7. *OsHSP60-3B* regulates the expression of genes related to reactive oxygen species (ROS) and heat stress response in rice anthers at high temperature. **A**, Overlap of differentially expressed genes (DEGs) in *oshsp60-3b* anthers compared with wild type at S10–12 at 34°C. **B**, Heat map showing expression of DEGs in WT and *oshsp60-3b* anthers at S10–12 at 34°C. Black color indicates downregulation, red color indicates upregulation. TPM: transcript per million. **C**, Gene Ontology (GO) pathway analysis of ROS-related DEGs in *oshsp60-3b* anthers. BP, biological process; MF, molecular function. GeneRatio is the percentage of DEGs in the GO term; P.adjust indicates significance level of enrichment.

also enriched at S12 (Fig. 7C). We selected 6 ROS-related, HSP, and HSF genes to verify results of RNA sequencing by RT-qPCR (Supplemental Fig. 10), which confirmed that these genes were substantially upregulated in *oshsp60-3b* compared with WT anthers at high temperatures, and also compared with expression in WT and mutant anthers at lower temperatures. These results indicated that *OsHSP60-3B* may affect male fertility by regulating the ROS process and/or expression of heat stress-related HSPs and HSFs.

RNA-seq data implied that *oshsp60-3b* anthers may accumulate excess ROS, which can produce oxidative damage and induce cell death. WT and *oshsp60-3b* anthers grown at 28°C and 34°C were collected, and stained separately with trypan blue to indicate cell death, and with DAB (3,3′-diaminobenzidine) to indicate peroxide accumulation (Fig. 8). The trypan blue assay revealed some difference between *oshsp60-3b* and WT S11 and S12 anthers grown at 28°C, but a much more marked difference at 34°C (Fig. 8, A and B), indicating that high temperature induced elevated cell death. The DAB assay indicated that *oshsp60-3b* anthers also accumulated much more H_2O_2 than WT anthers from S10–12, an effect that was again much higher at 34°C (Fig. 8, C and D). These results indicated that the more pronounced degradation of *oshsp60-3b* pollen at 34°C compared with 28°C (Figs. 2 and 3) is, in part, due to cell death caused by temperature-induced elevated ROS levels.

OsHSP60-3B overexpression can protect pollen against heat shock

HSP60 family proteins have been shown to protect plants from temperature-induced damage and stress (Qu et al. 2013; Ohama et al. 2017). We have shown that *OsHSP60-3B* expression increases under heat shock (Fig. 5D) and that the *oshsp60-3b* mutation increases susceptibility to heat (Fig. 8). To test whether overexpression of *OsHSP60-3B* could improve heat tolerance compared with WT, we generated three overexpression lines (OE1–3), and grew them at heat stress (36°C) conditions with WT plants.

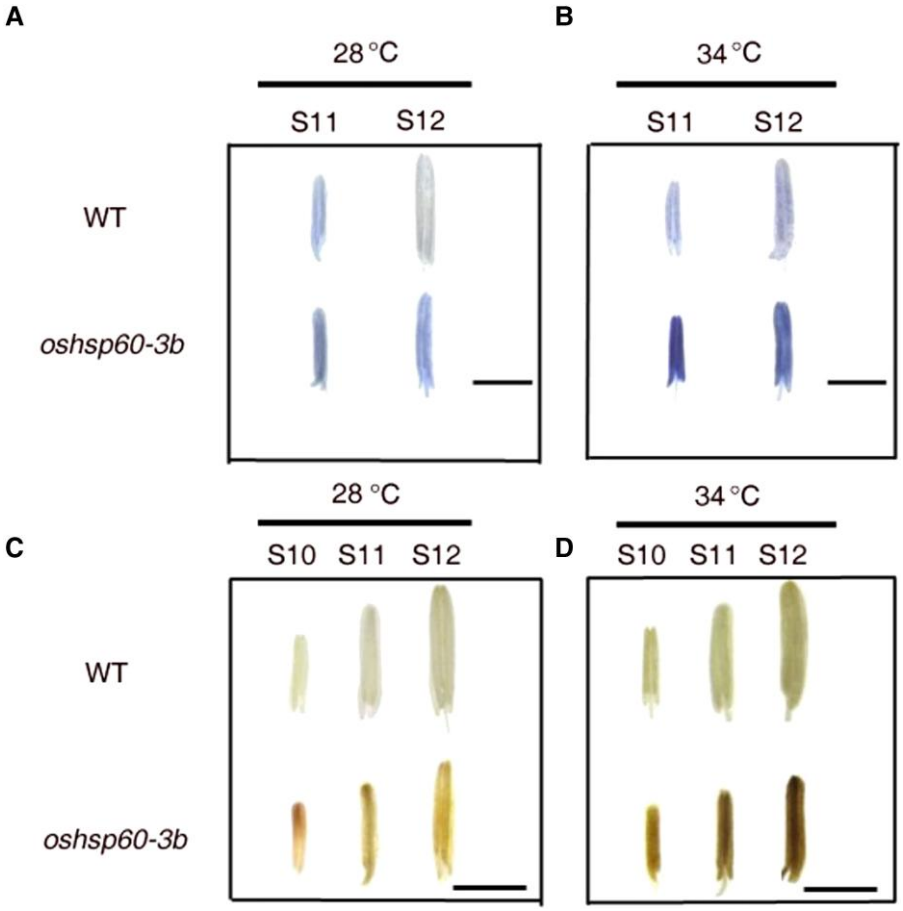

Figure 8. OsHSP60-3B suppresses cell death and H_2O_2 accumulation under heat stress (34°C). A and B, Trypan blue staining of WT and *oshsp60-3b* anthers at S11 and S12 at 28°C (**A**) and 34°C (**B**). Dark staining indicates cell death. Bars, 1 mm. Compared with wild type, *oshsp60-3b* plants accumulate much higher H_2O_2 in the anther at 34°C. **C** and **D**, DAB staining of WT and *oshsp60-3b* anthers at S10–12 at 28°C (**C**) and 34°C (**D**). Dark staining indicates H_2O_2 accumulation. Bars, 1 mm. Much stronger cell death signal is observed in *oshsp60-3b* anthers at 34°C.

Expression of *OsHSP60-3B* was detected in all plants, with much higher expression in the OE lines (Fig. 9A). Pollen viability in wild type was 9.87% and 15.97%, 22.60% and 20.40% in OE lines 1 to 3, respectively (Fig. 9, C, D, E, and F). Therefore, pollen viability was much higher in the OE lines, from 16% to 22%, compared with <10% in the WT line (Fig. 9B). These results reveal that *OsHSP60-3B* can improve heat tolerance of rice pollen.

Discussion

OsHSP60-3B is essential for pollen heat tolerance

Global warming is expected to increase the frequency of heat stress, which contributes massively to worldwide crop losses. It is of vital importance to generate heat-resilient crop varieties, especially those that can withstand stress during the extremely sensitive reproductive stages. Currently, very few genes capable of enhancing reproductive heat tolerance in rice have been reported but here, we show that *OsHSP60-3B* can improve the heat resilience of rice pollen.

The HSP/chaperone network is a major component of the heat stress response that deals with cellular protein homeostasis. The "chaperone titration model" suggests that HSFs are sequestered by HSP70/90 chaperones under optimal conditions and liberated by an increase in HSP clients (e.g. misfolded proteins) induced by heat stress and other stresses, triggering high HSP and HSF production (Guo et al. 2001; Zhang et al. 2022a). Unlike other HSPs, plant CPN60s/HSP60s are well known for their housekeeping roles in folding and aggregating many proteins transported to chloroplasts and mitochondria under normal conditions, but their role, if any, in heat stress response remains largely unknown. In rice, five of the six *OsCPN60* genes are induced by heat shock, particularly *OsCPN60α1* and *OsCPN60α2* (Kim et al. 2013). However, the *oscpn60α1* mutant plant does not exhibit heat sensitivity and overexpression of *OsCPN60α1* does not confer heat tolerance (Kim et al. 2013).

In this study, we have provided several lines of evidence that *OsHSP60-3B* is essential for heat tolerance of rice pollen. Firstly, *OsHSP60-3B* was strongly induced by heat shock within 0.25 h, indicating that *OsHSP60-3B* is a quick heat shock

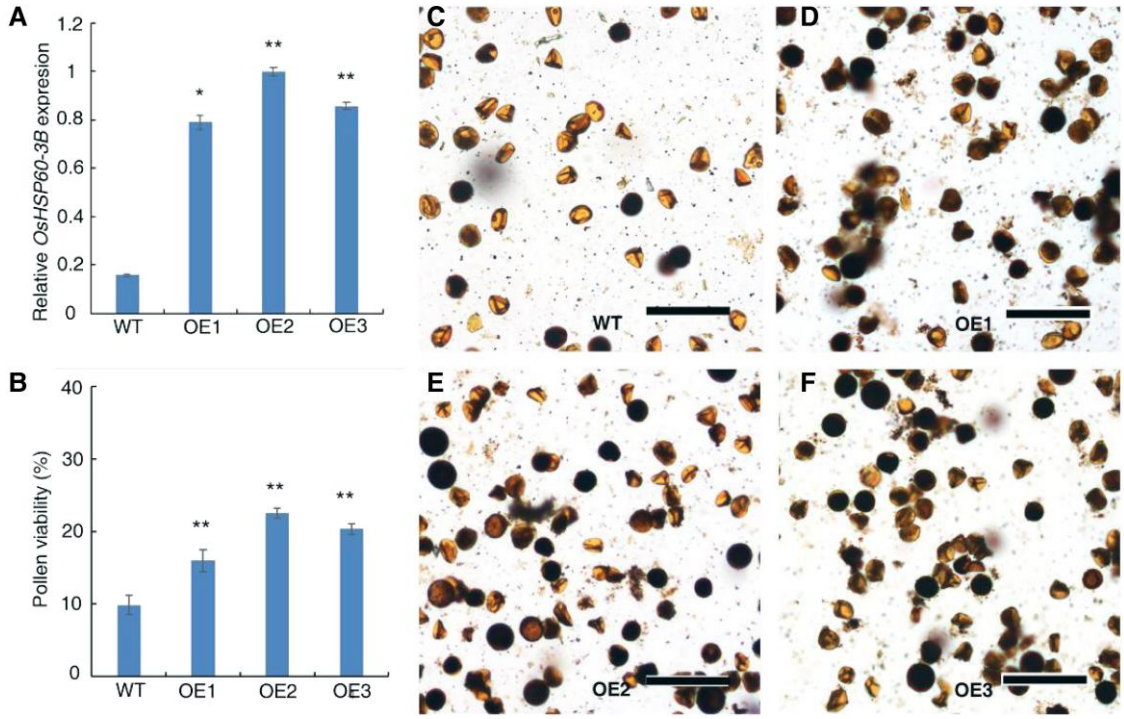

Figure 9. *OsHSP60-3B* overexpression improved heat tolerance at 36°C. **A**, Expression of *OsHSP60-3B* in the flag leaves of WT and three *OsHSP60-3B* overexpression (OE) plants in which OsHSP60-3B is driven by the maize Ubiquitin promoter, relative to OsActin. Mean ± SD, $n = 3$. * $P < 0.05$; ** $P < 0.01$ (Student's *t*-test). **B**, Pollen viability of WT and OsHSP60-3B OE plants grown at 36°C (3.5 h heat treatment in the middle of the day for 2 wk). Mean ± SD, $n = 3$. * $P < 0.05$; ** $P < 0.01$ (Student's *t*-test). **C** and **F**, WT (**C**) and OE (**D** to **F**) pollen grown at 36°C stained with I_2–KI. Dark staining indicates viable pollen. Bars, 100 μm.

response factor (Fig. 5D). Secondly, dysfunction of *OsHSP60-3B* caused male sterility at high temperatures (Fig. 1). Thirdly, overexpression of *OsHSP60-3B* enhanced the heat tolerance of pollen in transgenic plants (Fig. 9). In *oshsp60-3b* anthers, microspore abortion occurred after meiosis and tapetal programmed cell death was not affected (Fig. 2A; Supplemental Fig. S3), suggesting that *OsHSP60-3B* is specifically involved in the high temperature response during late anther development. Although ubiquitously expressed, *oshsp60-3b* plants did not exhibit obvious visible changes during vegetative growth (Supplemental Fig. S1A), suggesting that other rice HSP60 proteins may have redundant functions at these developmental stages. Taken together, our results show that *OsHSP60-3B* is a promising candidate for improving rice plant heat tolerance during reproductive growth.

OsHSP60-3B regulates starch granule biogenesis under high temperatures

Chloroplasts are remarkably dynamic plant plastids, which exist in various forms depending on developmental or environmental cues. CPN60s are known to be involved in the biogenesis and functioning of chloroplasts; they assist in the folding of several chloroplast proteins, such as the large Rubisco subunit (RbcL) and NdhH, a subunit of the chloroplast NADH dehydrogenase-like complex (NDH; Peng et al. 2011; Kim et al. 2013). However, the role of HSP60 chaperonins in the biogenesis of non-photosynthetic plastids has not previously been reported.

Our results indicate that OsHSP60-3B, targeted to plastids in rice and Arabidopsis protoplasts (Fig. 5E; Supplemental Fig. S8), is a key factor that mediates normal initiation and formation of starch granule (amyloplast) biogenesis in pollen at high temperatures. In *oshsp60-3b* mutants, starch granules looked normal at 22°C, but became smaller when grown at 28°C and are nearly abolished at 34°C (Fig. 3). In addition, the number of chloroplasts carrying no starch granules was increased and the size of starch granules was decreased in the anther endothecium cells at Stage 9 (Supplemental Fig. 11). This result suggests that starch synthesis in the mutant anther was also affected under high temperature, although not as severe as that in the pollen.

In rice, mature pollen grains accumulate starch to support pollen germination and pollen tube growth (Lee et al. 2016). Several proteins have been reported to play a role in the starch granule biogenesis in the rice pollen, including SUBSTANDARD STARCH GRAIN4 (SSG4), SUBSTANDARD STARCH GRAIN (SSG6), PLASTIDIC PHOSPHOGLUCOMUTASE (OsPGM), ADP-GLUCOSE PYROPHOSPHORYLASE LARGE SUBUNIT4 (OsAGPL4), UDP-GLUCOSE PYROPHOSPHORYLASE2 (OsUGP2), FLO6, and FLOURY ENDOSPERM (FLO7) (Mu et al. 2009;

Matsushima et al. 2014; Lee et al. 2016; Matsushima et al. 2016; Zhang et al. 2016, 2022b). FLO6 is the homolog of Arabidopsis PROTEIN TARGETING TO STARCH2 (PTST2), a protein containing a glucan-binding domain belonging to the CBM48 family. In Arabidopsis, PTST2 interacts with STARCH SYNTHASE4 (SS4), which is critical for the starch granule initiation and morphology in leaves (Seung et al. 2017). In rice, FLO6 interacts with ISOAMYLASE1 (ISA1), GRANULE-BOUND STARCH SYNTHASE I (GBSSI), GRANULE-BOUND STARCH SYNTHASEII (GBSSII), and STARCH SYNTHASE IVb (SSIVb), enzymes critical for starch granule initiation and development (Peng et al. 2014; Zhang et al. 2022b). Mutations in *FLO6* lead to defective starch granule formation in the endosperm and pollen, leading to decreased male fertility (Zhang et al. 2022b). We have demonstrated that OsHSP60-3B directly interacts with FLO6 (Fig. 6, A to C). OsHSP60-3B was evenly distributed in the plastid (Fig. 5E; Supplemental Fig. S8), suggesting that it is localized in the stroma, consistent with the localization of FLO6 reported previously (Zhang et al. 2022b). Furthermore, disruption of *OsHSP60-3B* destabilized FLO6 at high temperatures (Fig. 6D). In summary, these data suggest that OsHSP60-3B is an essential regulator of pollen starch granule biogenesis at high temperatures.

In Arabidopsis, homologs of *OsHSP60-3* have been reported to be localized in the mitochondria and participate in RNA splicing via interacting with What's This Factor 9 (WTF9), a nuclear-encoded plant organelle RNA recognition (PORR) protein (Hsu et al 2019). The distinct subcellular locations and functions of these homologs suggest functional divergence during evolution. Investigations into HSP60-3B homologs in other species will provide further insights into the function(s) of this HSP60 sub-family.

OsHSP60-3B is required to attenuate ROS levels in the anther

Production of ROS to deleterious levels is one of main negative consequences of heat stress. Excessive ROS accumulation can lead to lipid peroxidation, DNA damage, protein oxidation, and apoptosis (Scandalios 2005). Here, we observed a substantial increase in peroxide levels and apoptosis in *oshsp60-3b* compared with WT anthers at high temperature (Fig. 8), suggesting that OsHSP60-3B inhibits the overproduction of ROS and subsequent induction of cell death, thereby enhancing the resilience to heat stress.

The accumulation of ROS in response to stress occurs in multiple cellular compartments, and chloroplasts have been considered one of the major sites of ROS production. Exposure to heat stress can lead to the increased ROS accumulation in photosystem I (PSI), PSII, and the Calvin–Benson cycle, which causes irreversible oxidative damage to cells (Asada 2006; Suzuki et al. 2012). In the rice anthers, plastids in the endothecium develop into chloroplasts (Zhang et al. 2021). The rice anther is pale green when the panicle gradually emerges from the flag leaf, suggesting active photosynthetic activity. Therefore, it is highly possible that chloroplasts in the anther endothecium are the major producers of ROS during late anther development.

How OsHSP60-3B attenuates the ROS level in the anther is yet unknown. After chloroplasts sense heat stress, ROS and other signal molecules dependent on chloroplast retrograde signaling reprogram nuclear gene expression to activate a large array of heat stress response genes, including many molecular chaperones (Woodson and Chory 2008; Dickinson et al. 2018). Several chloroplast-targeted HSPs have been reported to enhance thermotolerance. For example, the Arabidopsis chloroplast-localized HSP100 protein APG6/ClpB3 reactivates the misfolded deoxyxylulose 5-phosphate synthase (DXS) to improve heat tolerance (Pulido et al. 2016), while the tomato (*Lycopersicon esculentum*) chloroplast-targeted LeHSP100/ClpB is thought to protect PSII from heat stress damage (Yang et al. 2006). A recent report demonstrates that, during heat stress, CPN60A guards the chloroplast ROS scavenger regulator thioredoxin-like 1 (TaRXL1) from degradation in Arabidopsis (Pant et al. 2020). It is possible that OsHSP60-3B is also involved in maintaining the homeostasis of the chloroplast photosynthetic or ROS scavenging machinery. Identification of other substrates of OsHSP60-3B in the future will shed light on the detailed mechanisms underlying ROS control.

In summary, we demonstrate the role of a rice HSP60 protein in thermotolerance during reproductive development. Our results suggest that the plastid-localized OsHSP60-3B is required for stabilizing starch granule biogenesis, and preventing ROS over-production in the anther at high temperatures. *OsHSP60-3B* may be a suitable target for breeding rice varieties with better tolerance to heat stress to meet the imminent challenges of a changing climate.

Materials and methods

Plant materials, growth conditions, and generation of *OsHSP60-3b* CRISPR lines

Rice (*Oryza sativa*) lines were generated in cultivar 9522 (*O. sativa ssp japonica*). The original *oshsp60-3b* male-sterile mutant was identified from an existing ^{60}Co γ-ray mutant library in cv. 9522 (Chen et al. 2006).

Rice plants were grown in the paddy field outside Shanghai Jiao Tong University in May every year until inflorescence length reached ~0.5 cm (Stage 3 (S3) of anther development; Zhang and Wilson 2009; Zhang et al. 2011), a proportion of the plants were kept in the paddy field, while another part of the plants were transferred to an artificial climate chamber for temperature and photoperiod treatments. Standard growth conditions (12 h light, 28°C, 75% relative humidity) were used to induce reproductive growth for ~2 wk, before plants were subjected to treatment at 75% relative humidity with 12 h light at low (22°C), mid (28°C), or high (34°C) temperatures, or heat stress at 14 h light/36°C (3.5 h at 42°C at noon time, (Supplemental Table S1). Short-term heat shock (3 h at 42°C) during early vegetative growth (2 wk seedlings) was used to generate leaves for gene expression analysis.

Genome editing technology was used to generate *oshsp60-3b-c1/c2* mutants using CRISPR/Cas9. Two target sequences (Supplemental Table S2) from exons 3 and 13 of *OsHSP60-3B* were designed using CRISPR-P v2.0 (http://cbi.hzau.edu.cn/CRISPR2/) and cloned into sgRNA-Cas9 vector for gene editing following Zhang et al (2014).

To construct *OsHSP60-3B* overexpression vectors, RNA from 9522 anthers at S10 was isolated and used to generate cDNA according to Liu et al. (2017). The *OsHSP60-3B* coding sequences was amplified and cloned into the overexpression vector PTCK303 under control of the *Ubiquitin* promoter (pUbi) using primers listed in Supplemental Table S8.

Both the gene editing and overexpression constructs were introduced into *Agrobacterium tumefaciens* strain EHA105, and used to transform rice callus induced from panicle at pre-meiotic stage according to Zhu et al. (2021).

Phenotypic characterization of *oshsp60-3b*

The morphology of whole plant and floral organs was recorded with a Nikon E995 digital camera. To observe pollen viability, wild-type (WT) and *oshsp60-3b* anthers were crushed with tweezers and stained with I_2–KI solution (0.2% (w/v) iodine, 2% (w/v) potassium iodide). Pollen grains released from anthers were observed through a Leica DM2500 microscope. Pollen viability was determined in spikelets from 10 independent plants for each genotype. Seed setting rate was calculated from panicles of 10 independent plants for each genotype.

Preparation and observation of semi-thin sections were performed as described previously (Li et al. 2006). TEM and SEM analyses were done as described previously (Liu et al. 2017).

Cloning of *OsHSP60-3b* and generation of complemented lines

Bulked segregation analysis (Liu et al. 2005) was used to map the *OsHSP60-3B* locus using InDel markers based on sequence differences between japonica and indica rice subspecies (http://www.ncbi.nlm.nih.gov). An F_2 population was generated from a cross between wild-type indica (GuangLuAi) and the original mutated japonica (*oshsp60-3b*) lines. *OsHSP60-3B* was first mapped between two InDel markers (AC087543 and AC069145). To further narrow the region, another 3 InDel markers (AC025905, AC068951-3, and AC022457) were designed and used, and *OsHSP60-3B* was finally mapped to between AC068951-3 and AC022457. Primers used in the map-based cloning are listed in Supplemental Table S8.

High-throughput sequencing of *oshsp60-3b* was applied to the mixed F_2 population. An 8 bp deletion in exon 17 of LOC_Os10g32550 was found to cause a frame shift. To verify this gene was responsible for the *oshsp60-3b* phenotype, an 8.8 kb genomic fragment containing a 2.9 kb upstream promoter region, 5.0 kb *OsHSP60-3B* coding region, and 870 bp downstream region was amplified from BAC clone OSJNBa0071K18 containing *OsHSP60-3B*. The genomic fragment was inserted into the pCAMBIA1301 vector and transformed into *oshsp60-3b* rice callus using *Agrobacterium*-mediated transformation, as described above. PCR was used to identify positive transgenic lines for subsequent complementation analysis. Primers used for vector construction are listed in Supplemental Table S8.

Reverse transcription quantitative PCR (RT-qPCR) and GUS staining assays

Total RNA was extracted from different tissues including root, stem, leaf at seedling stage, palea/lemma at maturity, and anthers at Stages 6 to 13 of development using Trizol (Invitrogen) according to manufacturer's instructions. RNA (1 μg) was used to synthesize cDNA using the Primescript RT reagent kit (Takara Bio) according to manufacturer's instructions. RT-qPCR analyses were performed in the Bio-Rad C1000 thermal cycler using QuantiNova SYBR Green PCR Kit (QIAGEN) according to manufacturer's instructions. OsActin (LOC_Os3g50885) was used as the internal standard, and data analysis was performed as previously described (Yu et al 2017). Primers used for PCR amplification are listed in Supplemental Table S8.

The 2.9 kb *OsHSP60-3B* promoter was cloned into pCAMBIA 1301 vector containing the GUS (*β-glucuronidase*) reporter gene. The *pOsHSP60-3B::GUS* construct was transformed into wild type cv. 9522 by *Agrobacterium*-mediated tissue transformation as described above. Mature spikelets of the positive transgenic line were immersed in X-Gluc (5-bromo-4-chloro-3-indolyl β-D-glucuronide) solution at 37 °C overnight in the dark until color developed. Tissues were washed in 70% (v/v) ethanol and photographed with a phase-contrast microscope (Leica DM2500). Primers used for vector construction are listed in Supplemental Table S8.

Phylogenetic analysis

The protein sequence of the OsHSP60-3B TCP1 domain was used for a BLASTp search for homologous sequences in Phytozome (https://phytozome-next.jgi.doe.gov/). Fourteen Arabidopsis (*Arabidopsis thaliana*) and 10 rice homologs were found and used for sequence alignment. A phylogenetic tree based on the TCP1-1/CPN60 chaperonin domain sequences was generated with MEGA5 software, using the Neighbor-Joining method with Poisson correction, pairwise deletion, and 1,000 bootstrap replicates.

Subcellular localization of OsHSP60-3B

Full-length *OsHSP60-3B* cDNA was cloned into pA7-eGFP vector to generate *p35S::OsHSP60-3BCDS-eGFP* (primers listed in Supplemental Table S8) for transient expression. The construct and empty vector were separately transformed into Arabidopsis and rice protoplasts derived from stem tissue of etiolated WT seedlings using polyethylene glycol-mediated transformation (Bart et al. 2006; Yoo et al. 2007).

Fluorescence signals were observed under a confocal laser-scanning microscopy (Leica TCS SP5, excitation 488 nm, emission 500 to 550 nm for eGFP; excitation 488 nm, emission 650 to 750 nm for chlorophyll autofluorescence).

Cell physiology

For 4′,6-diamidino-2-phenylindole (DAPI) staining assays at 34°C, young spikelets collected from meiotic stages were fixed with Carnoy's solution (ethanol:glacial acetic 3:1 [v/v]), and then prepared as described previously (Zhang et al. 2019).

Cell death and H_2O_2 accumulation were measured by trypan blue and 3,3′-diaminobenzidine (DAB) staining, respectively. Trypan blue staining was prepared as previously described (Wu et al. 2015). Briefly, WT and mutant anthers at Stages 10 and 11 grown at 28°C and 34°C were covered with a trypan blue solution (30 ml ethanol, 10 g phenol, 10 ml water, 10 ml glycerol, 10 ml lactic acid, and 10 mg trypan blue), boiled for 2 to 3 min, and incubated at room temperature for 1 h. To destain, the samples were transferred into a chloral hydrate solution (2.5 g ml^{-1}) and boiled for 20 min several times. The samples were equilibrated with 50% (v/v) glycerol, mounted, and imaged with a Nikon E995 digital camera.

DAB (D5637, Sigma-Aldrich) staining was performed as described by Wu et al. (2015). Briefly, WT and mutant anthers at Stage 10 and 11 grown at 28°C and 34°C were immersed in freshly prepared 1 mg ml^{-1} DAB solution (pH 3.8) and infiltrated under vacuum. Stained samples were boiled in 1:1:3 acetic acid: glycerol: ethanol, stored under 95% (v/v) ethanol, and photographed with a Nikon E995 digital camera.

Analysis of protein–protein interactions

To screen for OsHSP60-3B interactive proteins, cDNA synthesized from the mRNAs of anthers (5 to 7 mm) was cloned into the prey vector pGADT7, and full length of OsHSP60-3B cDNA was amplified and cloned into pGBKT7 vector. Yeast library screening was conducted as per instructions of the Matchmaker™ Library Construction & Screening Kits (Clontech).

For yeast two-hybrid assays, FLO6 constructs were kindly provided by Prof. Cunxu Wei. The full-length WT *OsHSP60-3B* coding sequences was cloned into EcoRI and BamHI restriction sites of pGADT7 and pGBKT7 vectors encoding the GAL4 activation domain (AD) or binding domain (BD), respectively. Plasmids were co-transformed into yeast (*Saccharomyces cerevisiae*) strain AH109, according to the manufacturer's instructions (TaKaRa). Transformants were selected on SD medium -LT (-Leu/-Trp), while protein–protein interactions were selected on SD medium -LTHA (-Leu/-Trp/-His/-Ade) as previously described (Cao et al. 2021).

For split-luciferase assays, full-length *OsHSP60-3B* and *FLO6* coding sequences were cloned separately into the pCAMBIA 1300-nLuc and 1300-cLuc plasmids, encoding the N-terminal and C-terminal luciferase domains, respectively. Constructs were transiently transformed into *Agrobacterium tumefaciens* GV3101 as described above. The bacteria were resuspended in infection solution (10 mM MES, 10 mM $MgCl_2$, and 200 μM acetosyringone) and infiltrated into 4-wk-old *Nicotiana tabacum* leaves. After 36 h incubation in the dark, leaves were sprayed with 5 mM luciferin and photographed with a Tanon 5200 Chemiluminescent Imaging System.

For bimolecular fluorescence complementation assays, full-length *OsHSP60-3B* and *FLO6* coding sequences separately cloned into the pXY106-nYFP or pXY104-cYFP plasmids, containing N-terminal and C-terminal yellow fluorescent protein domains, respectively. Constructs were transiently transformed into 4-wk-old *Nicotiana tabacum* leaves as described above. After 36 h incubation in the dark, fluorescent YFP signals were captured using a Leica SP5 confocal microscope (Leica TCS SP5, excitation 514 nm; emission 522 to 555 nm). Primers used for all protein–protein interaction assays are listed in Supplemental Table S8.

RNA-seq and Gene Ontology (GO) enrichment analysis

Total RNA was extracted in duplicate from WT and *oshsp60-3b* anthers grown at 34°C at Stages 10, 11, and 12, and sequenced with the DNBSeq platform (BGI, Shenzhen). Differentially expressed genes (DEGs) were determined by DEseq2, using $|\log_2 \text{fold change}| \geq 1$ and $q < 0.05$ (Audic and Claverie 1997) after gene alignment and filtering of low-quality reads (Sun et al. 2021). Rpackage "pheatmap" (Sun et al. 2021) was used to create and analyze heatmaps and dendrograms of gene expression using the k-means clustering algorithm. The AgriGo2 algorithm was used to analyze the results of Gene Ontology (GO) enrichment, and data were screened by false discovery rate (FDR) < 0.05 (Tian et al. 2017). GO enrichment results were visualized by Rpackage "Clusterprofiler" (Yu et al. 2012a).

Statistical analysis

All data from RT-qPCR experiments were obtained from three independent biological replicates. The data for pollen viability and seed setting rate at 22°C, 28°C, and 34°C were obtained from 10 independent biological replicates. The data for pollen viability at 36°C were obtained from three independent biological replicates. Data were plotted as mean ± standard deviation (SD). The data were analyzed with the two-tailed Student's *t*-test using Microsoft Excel 2010.

Accession numbers

Sequence data from this article can be found in the GenBank/EMBL data libraries under accession numbers PRJNA933966. The accession numbers of the major genes/proteins mentioned are listed in Supplemental Table S9.

Author contributions

W.L. designed the project. S.L., Z.L., L.Z., S.S., F.X., H.L., A.T., and L.C. performed all the experiments. S.L., Z.L., Z.A.W., D.Z., and W.L. wrote the manuscript. All authors discussed the results and commented on the article.

Supplemental data

The following materials are available in the online version of this article.

Supplemental Figure S1. Rice *hsp60-3b* mutants exhibit partial male sterility in the field (25 to 32°C).

Supplemental Figure S2. F1 progeny exhibited a normal phenotype.

Supplemental Figure S3. Disruption of *OsHSP60-3B* does not affect meiosis progression in the anther at 34°C.

Supplemental Figure S4. Disruption of *OsHSP60-3B* does not affect the development of anthers, tapetal cells, and microspores at Stages 8 to 10 at high temperature (34°C).

Supplemental Figure S5. The cuticle, Ubisch body, and pollen exine formation are normal in *oshsp60-3b*.

Supplemental Figure S6. *OsHSP60-3B* is required for rice male fertility at high temperatures.

Supplemental Figure S7. Complementation of *oshsp60-3b* with *pOsHSP60-3B::OsHSP60-3B* gDNA at 34°C.

Supplemental Figure S8. OsHSP60-3B is localized to plastids in Arabidopsis protoplasts.

Supplemental Figure S9. Heat map showing expression of HSP and HSF DEGs in WT and oshsp60-3b anthers at S10–12 at 34°C.

Supplemental Figure S10. The expression of genes related to HSP, HSF, and ROS generation were up-regulated in S11 oshsp60-3b mutant anthers compared with WT at 34°C.

Supplemental Figure S11. Starch granules in the endothecium chloroplasts of anther at 34°C.

Supplemental Table S1. Low, mid, high temperature and heat stress treatment of WT and *oshsp60-3b* plants at 75% relative humidity.

Supplemental Table S2. Differentially expressed genes in *oshsp60-3b* anthers at Stage 10 compared to the wild type at 34°C.

Supplemental Table S3. Differentially expressed genes in *oshsp60-3b* anthers at Stage 11 compared to the wild type at 34°C.

Supplemental Table S4. Differentially expressed genes in *oshsp60-3b* anthers at Stage 12 compared to the wild type at 34°C.

Supplemental Table S5. GO enrichment in *oshsp60-3b* anthers at Stage 10 compared to the wild type.

Supplemental Table S6. GO enrichment in *oshsp60-3b* anthers at Stage 11 compared to the wild type.

Supplemental Table S7. GO enrichment in *oshsp60-3b* anthers at Stage 12 compared to the wild type.

Supplemental Table S8. Primers used for experiments.

Supplemental Table S9. Accession numbers of the major genes/proteins.

Acknowledgments

The authors thank Dr Natalie Betts for editing this manuscript; Ms Mingjiao Chen, Mr Zhijing Luo, Mr Ting Luo, and Mr Zibo Chen for rice plant growth and fieldwork; Ms Xiaofei Chen for rice transformation; and Mr Jie Zhang for help in dapi experiment.

Funding

This work was supported by the Guangdong Basic and Applied Basic Research Foundation (2022B1515120036), the National Natural Science Foundation of China (U19A2031 and 31871585), Special Funds for Construction of Innovative Provinces in Hunan Province (2021NK1002), the China Postdoctoral Science Foundation (2019M 651483), and the Royal Society (CHL\R1\180496 - Challenge-led Grants 2018).

Conflict of interest statement. None declared.

References

Apuya NR, Yadegari R, Fischer RL, Harada JJ, Lynn Zimmerman J, Goldberg R. The Arabidopsis embryo mutant *schlepperless* has a defect in the *Chaperonin-60α* gene. Plant Physiol. 2001:**126**(2): 717–730. https://doi.org/10.1104/pp.126.2.717

Asada K. Production and scavenging of reactive oxygen species in chloroplasts and their functions. Plant Physiol. 2006:**141**(2): 391–396. https://doi.org/10.1104/pp.106.082040

Audic S, Claverie JM. The significance of digital gene expression profiles. Genome Res. 1997:**7**(10): 986–995. https://doi.org/10.1101/gr.7.10.986

Bart R, Chern M, Park CJ, Bartley L, Ronald PC. A novel system for gene silencing using siRNAs in rice leaf and stem-derived protoplasts. Plant Methods. 2006:**2**(1): 13. https://doi.org/10.1186/1746-4811-2-13

Cao L, Tian J, Liu Y, Chen X, Li S, Persson S, Lu D, Chen M, Luo Z, Zhang D, et al. Ectopic expression of OsJAZ6, which interacts with OsJAZ1, alters JA signaling and spikelet development in rice. Plant J. 2021:**108**(4): 1083–1096. https://doi.org/10.1111/tpj.15496

Chaturvedi P, Wiese AJ, Ghatak A, Záveská Drábková L, Weckwerth W, Honys D. Heat stress response mechanisms in pollen development. New Phytol. 2021:**231**(2): 571–585. https://doi.org/10.1111/nph.17380

Chen L, Chu HW, Yuan Z, Pan AH, Liang WQ, Huang H, Shen MS, Zhang DB, Chen L. Isolation and genetic analysis for rice mutants treated with ^{60}Co c-ray. J Xiamen Univ. 2006:**45**(1): 82–85. https://doi.org/10.3321/j.issn:0438-0479.2006.z1.021

Chen ZL, Galli M, Gallavotti A. Mechanisms of temperature-regulated growth and thermotolerance in crop species. Curr Opin Plant Biol. 2022:**65**: 102134. https://doi.org/10.1016/j.pbi.2021.102134

Crafts-Brandner SJ, Salvucci ME. Rubisco activase constrains the photosynthetic potential of leaves at high temperature and CO_2. Proc Natl Acad Sci U S A. 2000:**97**(24): 13430–13435. https://doi.org/10.1073/pnas.230451497

De Storme N, Geelen D. The impact of environmental stress on male reproductive development in plants: biological processes and molecular mechanisms. Plant Cell Environ. 2014:**37**(1): 1–18. https://doi.org/10.1111/pce.12142

Dickinson PJ, Kumar M, Martinho C, Yoo SJ, Lan H, Artavanis G, Charoensawan V, Schöttler MA, Bock R, Jaeger KE, et al. Chloroplast signaling gates thermotolerance in Arabidopsis. Cell Rep. 2018:**22**(7): 1657–1665. https://doi.org/10.1016/j.celrep.2018.01.054

Finka A, Mattoo RU, Goloubinoff P. Experimental milestones in the discovery of molecular chaperones as polypeptide unfolding enzymes. Annu Rev Biochem. 2016:**85**(1): 715–742. https://doi.org/10.1146/annurev-biochem-060815-014124

Firon N, Shaked R, Peet MM, Pharr DM, Zamski E, Rosenfeld K, Althan L, Pressman E. Pollen grains of heat tolerant tomato cultivars

retain higher carbohydrate concentration under heat stress conditions. Sci Hortic. 2006:**109**(3): 212–217. https://doi.org/10.1016/j.scienta.2006.03.007

Guo Y, Guettouche T, Fenna M, Boellmann F, Pratt WB, Toft DO, Smith DF, Voellmy R. Evidence for a mechanism of repression of *HEAT SHOCK FACTOR 1* transcriptional activity by a multichaperone complex. J Biol Chem. 2001:**276**(49): 45791–45799. https://doi.org/10.1074/jbc.M105931200

Hafidh S, Fíla J, Honys D. Male gametophyte development and function in angiosperms: a general concept. Plant Reprod. 2016:**29**(1-2): 31–51. https://doi.org/10.1007/s00497-015-0272-4

Hemmingsen SM, Woolford C, van der Vies SM, Tilly K, Dennis DT, Georgopoulos CP, Hendrix RW, Ellis RJ. Homologous plant and bacterial proteins chaperone oligomeric protein assembly. Nature. 1988:**333**(6171): 330–334. https://doi.org/10.1038/333330a0

Hill JE, Hemmingsen SM. *Arabidopsis thaliana* type I and II chaperonins. Cell Stress Chaperones. 2001:**6**(3): 190–200. https://doi.org/10.1379/1466-1268(2001)006<0190:attiai>2.0.co;2

Hsu Y-W, Juan C-T, Wang C-M, Jauh G-Y. Mitochondrial heat shock protein 60 s interact with What's This Factor 9 to regulate RNA splicing of ccmFC and rpl2. Plant Cell Physiol. 2019:**60**(1): 116–125. https://doi.org/10.1093/pcp/pcy199

Ji S, Siegel A, Shan S, Grimm B, Wang P. Chloroplast SRP43 autonomously protects chlorophyll biosynthesis proteins against heat shock. Nat Plants. 2021:**7**(10): 1420–1432. https://doi.org/10.1038/s41477-021-00994-y

Jiang Q, Mei J, Gong X-D, Xu J-L, Zhang J-H, Teng S, Lin D-Z, Dong Y-J. Importance of the rice *TCD9* encoding α subunit of chaperonin protein 60 (Cpn60α) for the chloroplast development during the early leaf stage. Plant Sci. 2014:**215-216**: 172–9. https://doi.org/10.1016/j.plantsci.2013.11.003

Ke X, Zou W, Ren Y, Wang Z, Li J, Wu X, Zhao J. Functional divergence of chloroplast Cpn60α subunits during Arabidopsis embryo development. PLoS Genet. 2017:**13**(9): e1007036. https://doi.org/10.1371/journal.pgen.1007036

Kim S-R, Yang J-I, An G. *Oscpn60α1*, encoding the plastid chaperonin 60α subunit, is essential for folding of RbcL. Mol Cells. 2013:**35**(5): 402–409. https://doi.org/10.1007/s10059-013-2337-2

Larkindale J, Knight MR. Protection against heat stress-induced oxidative damage in Arabidopsis involves calcium, abscisic acid, ethylene, and salicylic acid. Plant Physiol. 2002:**128**(2): 682–695. https://doi.org/10.1104/pp.010320

Lee S-K, Eom J-S, Hwang S-K, Shin D, An G, Okita TW, Jeon J-S. Plastidic phosphoglucomutase and ADP-glucose pyrophosphorylase mutants impair starch synthesis in rice pollen grains and cause male sterility. J Exp Bot. 2016:**67**(18): 5557–5569. https://doi.org/10.1093/jxb/erw324

Li N, Zhang D-S, Liu H-S, Yin C-S, Li X, Liang W, Yuan Z, Xu B, Chu H-W, Wang J, et al. The rice *TAPETUM DEGENERATION RETDARDATION* gene is required for tapetum degradation and anther development. Plant Cell. 2006:**18**(11): 2999–3014. https://doi.org/10.1105/tpc.106.044107

Liu H, Chu H, Li H, Wang H, Wei J, Li N, Ding S, Huang H, Ma H, Huang C, et al. Genetic analysis and mapping of rice (*Oryza sativa L.*) male-sterile (OsMS-L) mutant. Chinese Sci Bull. 2005:**50**(2): 122–125. https://doi.org/10.1007/BF02897514

Liu Z, Lin S, Shi J, Yu J, Zhu L, Yang X, Zhang D, Liang W. *RICE NO POLLEN 1 (NP1)* is required for anther cuticle formation and pollen exine patterning. Plant J. 2017:**91**(2): 263–277. https://doi.org/10.1111/tpj.13561

Lohani N, Singh MB, Bhalla PL. High temperature susceptibility of sexual reproduction in crop plants. J Exp Bot. 2020:**71**(2): 555–568. https://doi.org/10.1093/jxb/erz426

Matsushima R, Maekawa M, Kusano M, Kondo H, Fujita N, Kawagoe Y, Sakamoto W. Amyloplast-localized SUBSTANDARD STARCH GRAIN4 protein influences the size of starch grains in rice endosperm. Plant Physiol. 2014:**164**(2): 623–636. https://doi.org/10.1104/pp.113.229591

Matsushima R, Maekawa M, Kusano M, Tomita K, Kondo H, Nishimura H, Crofts N, Fujita N, Sakamoto W. Amyloplast membrane protein SUBSTANDARD STARCH GRAIN6 controls starch grain size in rice endosperm. Plant Physiol. 2016:**170**(3): 1445–1459. https://doi.org/10.1104/pp.15.01811

Mu H, Ke J, Liu W, Zhuang C, Yip W. *UDP-GLUCOSE PYROPHOSPHORYLASE2* (OsUGP2), a pollen-preferential gene in rice, plays a critical role in starch accumulation during pollen maturation. Chinese Sci Bull. 2009:**54**(2): 234–243. https://doi.org/10.1007/s11434-008-0568-y

Ohama N, Sato H, Shinozaki K, Yamaguchi-Shinozaki K. Transcriptional regulatory network of plant heat stress response. Trends Plant Sci. 2017:**22**(1): 53–65. https://doi.org/10.1016/j.tplants.2016.08.015

Pant BD, Oh S, Lee H-K, Nandety RS, Mysore KS. Antagonistic regulation by *CPN60A* and *CLPC1* of *TRXL1* that regulates MDH activity leading to plant disease resistance and thermotolerance. Cell Rep. 2020:**33**(11): 108512. https://doi.org/10.1016/j.celrep.2020.108512

Peng L, Fukao Y, Myouga F, Motohashi R, Shinozaki K, Shikanai T. A chaperonin subunit with unique structures is essential for folding of a specific substrate. PLoS Biol. 2011:**9**(4): e1001040. https://doi.org/10.1371/journal.pbio.1001040

Peng S, Huang J, Sheehy JE, Laza RC, Visperas RM, Zhong X, Centeno GS, Khush GS, Cassman KG. Rice yields decline with higher night temperature from global warming. Proc Natl Acad Sci U S A. 2004:**101**(27): 9971–9975. https://doi.org/10.1073/pnas.0403720101

Peng C, Wang Y, Liu F, Ren Y, Zhou K, Lv J, Zheng M, Zhao S, Zhang L, Wang C, et al. FLOURY ENDOSPERM 6 encodes a CBM48 domain-containing protein involved in compound granule formation and starch synthesis in rice endosperm. Plant J. 2014:**77**(6): 917–930. https://doi.org/10.1111/tpj.12444

Pressman E. The effect of heat stress on tomato pollen characteristics is associated with changes in carbohydrate concentration in the developing anthers. Ann Bot. 2002:**90**(5): 631–636. https://doi.org/10.1093/aob/mcf240

Pulido P, Llamas E, Llorente B, Ventura S, Wright LP, Rodríguez-Concepción M. Specific HSP100 chaperones determine the fate of the first enzyme of the plastidial isoprenoid pathway for either refolding or degradation by the stromal Clp protease in Arabidopsis. PLoS Genet. 2016:**12**(1): e1005824. https://doi.org/10.1371/journal.pgen.1005824

Qu A-L, Ding Y-F, Jiang Q, Zhu C. Molecular mechanisms of the plant heat stress response. Biochem Biophys Res Commun. 2013:**432**(2): 203–207. https://doi.org/10.1016/j.bbrc.2013.01.104

Sangwan V, Orvar BL, Beyerly J, Hirt H, Dhindsa RS. Opposite changes in membrane fluidity mimic cold and heat stress activation of distinct plant MAP kinase pathways. Plant J. 2002:**31**(5): 629–638. https://doi.org/10.1046/j.1365-313X.2002.01384.x

Scandalios JG. Oxidative stress: molecular perception and transduction of signals triggering antioxidant gene defenses. Braz J Med Biol Res. 2005:**38**(7): 995–1014. https://doi.org/10.1590/S0100-879X2005000700003

Seung D, Boudet J, Monroe J, Schreier TB, David LC, Abt M, Lu KJ, Zanella M, Zeeman SC. Homologs of PROTEIN TARGETING TO STARCH control starch granule initiation in Arabidopsis leaves. Plant Cell. 2017:**29**(7): 1657–1677. https://doi.org/10.1105/tpc.17.00222

Song P, Jia Q, Chen L, Jin X, Xiao X, Li L, Chen H, Qu Y, Su Y, Zhang W, et al. Involvement of Arabidopsis phospholipase D δ in regulation of ROS-mediated microtubule organization and stomatal movement upon heat shock. J Exp Bot. 2020:**71**(20): 6555–6570. https://doi.org/10.1093/jxb/eraa359

Sun S, Wang D, Li J, Lei Y, Li G, Cai W, Zhao X, Liang W, Zhang D. Transcriptome analysis reveals photoperiod-associated genes

expressed in rice anthers. Front Plant Sci. 2021:**12**: 621561. https://doi.org/10.3389/fpls.2021.621561

Suzuki N, Koussevitzky S, Mittler R, Miller G. ROS and redox signalling in the response of plants to abiotic stress. Plant Cell Environ. 2012: **35**(2): 259–270. https://doi.org/10.1111/j.1365-3040.2011.02336.x

Suzuki K, Nakanishi H, Bower J, Yoder DW, Osteryoung KW, Miyagishima S. Plastid chaperonin proteins Cpn60 alpha and Cpn60 beta are required for plastid division in *Arabidopsis thaliana*. BMC Plant Biol. 2009:**9**(1): 38. https://doi.org/10.1186/1471-2229-9-38

Tashiro T, Wardlaw IF. A comparison of the effect of high temperature on grain development in wheat and rice. Ann Bot. 1989:**64**(1): 59–65. https://doi.org/10.1093/oxfordjournals.aob.a087808

Tian T, Liu Y, Yan H, You Q, Yi X, Du Z, Xu W, Su Z. AgriGO v2.0: a GO analysis toolkit for the agricultural community, 2017 update. Nucleic Acid Res. 2017:**45**(W1): W122–W129. https://doi.org/10.1093/nar/gkx382

Tissieres A, Mitchell HK, Tracy UM. Protein synthesis in salivary glands of *Drosophila melanogaster*: relation to chromosome puffs. J Mol Biol. 1974:**84**(3): 389–398. https://doi.org/10.1016/0022-2836(74)90447-1

Tiwari LD, Grover A. Cpn60β4 protein regulates growth and developmental cycling and has bearing on flowering time in *Arabidopsis thaliana* plants. Plant Sci. 2019:**286**: 78–88. https://doi.org/10.1016/j.plantsci.2019.05.022

Usman MG, Rafi MY, Ismail MR, Malek MA, Latif MA, Oladosu Y. Heat shock proteins: functions and response against heat stress in plants. Int J Sci Technol Res. 2014:**3**(11): 204–218

Wang Z, Li H, Liu X, He Y, Zeng H. Reduction of pyruvate orthophosphate dikinase activity is associated with high temperature-induced chalkiness in rice grains. Plant Physiol Biochem. 2015:**89**: 76–84. https://doi.org/10.1016/j.plaphy.2015.02.011

Woodson JD, Chory J. Coordination of gene expression between organellar and nuclear genomes. Nat Rev Genet. 2008:**9**(5): 383–395. https://doi.org/10.1038/nrg2348

Wu J, Sun Y, Zhao Y, Zhang J, Luo L, Li M, Wang J, Yu H, Liu G, Yang L, et al. Deficient plastidic fatty acid synthesis triggers cell death by modulating mitochondrial reactive oxygen species. Cell Res. 2015:**25**(5): 621–633. https://doi.org/10.1038/cr.2015.46

Wu Q, Zhang C, Chen Y, Zhou K, Zhan Y, Jiang D. *Oscpn60β1* is essential for chloroplast development in rice (*Oryza sativa* L.). Int J Mol Sci. 2020:**21**(11): 4023. https://doi.org/10.3390/ijms21114023

Yang J, Sun Y, Sun A, Yi S, Qin J, Li M, Liu J. The involvement of chloroplast HSP100/ClpB in the acquired thermotolerance in tomato. Plant Mol Biol. 2006:**62**(3): 385–395. https://doi.org/10.1007/s11103-006-9027-9

Yoo S, Cho Y, Sheen J. Arabidopsis mesophyll protoplasts: a versatile cell system for transient gene expression analysis. Nat Protoc. 2007:**2**(7): 1565–1572. https://doi.org/10.1038/nprot.2007.199

Yu J, Han J, Kim Y, Song M, Yang Z, He Y, Fu R, Luo Z, Hu J, Liang W, et al. Two rice receptor-like kinases maintain male fertility under changing temperatures. Proc Natl Acad Sci U S A. 2017:**114**(46): 12327–12332. https://doi.org/10.1073/pnas.1705189114

Yu G, Wang L-G, Han Y, He Q-Y. Clusterprofiler: an R package for comparing biological themes among gene clusters. OMICS. 2012a:**16**(5): 284–287. https://doi.org/10.1089/omi.2011.0118

Yu H-D, Yang X-F, Chen S-T, Wang Y-T, Li J-K, Shen Q, Liu X-L, Guo F-Q. Downregulation of chloroplast *RPS1* negatively modulates nuclear heat-responsive expression of *HSFA2* and its target genes in Arabidopsis. PLoS Genet. 2012b:**8**(5): e1002669. https://doi.org/10.1371/journal.pgen.1002669

Zhang W, Li H, Xue F, Liang W. Rice *GlUCOSE 6-PHOSPHATE/PHOSPHATE TRANSLOCATOR 1* is required for tapetum function and pollen development. Crop J. 2021:**9**(6): 1278–1290. https://doi.org/10.1016/j.cj.2021.03.010

Zhang L, Li N, Zhang J, Zhao L, Qiu J, Wei C. The CBM48 domain-containing protein FLO6 regulates starch synthesis by interacting with SSIVb and GBSS in rice. Plant Mol Biol. 2022b:**108**(4-5): 343–361. https://doi.org/10.1007/s11103-021-01178-0

Zhang D, Luo X, Zhu L. Cytological analysis and genetic control of rice anther development. J Genet Genomics. 2011:**38**(9): 379–390. https://doi.org/10.1016/j.jgg.2011.08.001

Zhang L, Ren Y, Lu B, Yang C, Feng Z, Liu Z, Chen J, Ma W, Jiang L, Wan J, et al. *FLOURY ENDOSPERM 7* encodes a regulator of starch synthesis and amyloplast development essential for peripheral endosperm development in rice. J Exp Bot. 2016:**67**(3): 633–647. https://doi.org/10.1093/jxb/erv469

Zhang J, Wang C, Higgins JD, Kim Y-J, Moon S, Jung K-H, Qu S, Liang W. A multiprotein complex regulates interference-sensitive crossover formation in rice. Plant Physiol. 2019:**181**(1): 221–235. https://doi.org/10.1104/pp.19.00082

Zhang D, Wilson ZA. Stamen specification and anther development in rice. Chinese Sci Bull. 2009:**54**(14): 2342–2353. https://doi.org/10.1007/s11434-009-0348-3

Zhang H, Zhang J, Wei P, Zhang B, Gou F, Feng Z, Mao Y, Yang L, Zhang H, Xu N, et al. The CRISPR/Cas9 system produces specific and homozygous targeted gene editing in rice in one generation. Plant Biotechnol J. 2014:**12**(6): 797–807. https://doi.org/10.1111/pbi.12200

Zhang H, Zhu J, Gong Z, Zhu J. Abiotic stress responses in plants. Nat Rev Genet. 2022a:**23**(2): 104–119. https://doi.org/10.1038/s41576-021-00413-0

Zhu W, Yang L, Wu D, Meng Q, Deng X, Huang G, Zhang J, Chen X, Ferrandiz C, Liang W, et al. Rice *SEPALLATA* genes *OsMADS5* and *OsMADS34* cooperate to limit inflorescence branching by repressing the *TERMINAL FLOWER1-LIKE* gene *RCN4*. New Phytol. 2021:**233**(4): 1682–1700. https://doi.org/10.1111/nph.17855

Zininga T, Ramatsui L, Shonhai A. Heat shock proteins as immunomodulants. Molecules. 2021:**23**(11): 2846. https://doi.org/10.3390/molecules23112846

Zinn KE, Tunc-Ozdemir M, Harper JF. Temperature stress and plant sexual reproduction: uncovering the weakest links. J Exp Bot. 2010:**61**(7): 1959–1968. https://doi.org/10.1093/jxb/erq053